Available online at www.sciencedirect.com
SCIENCE DIRECT®
Journal of Chromatography A, 1006 (2003) 61–76
JOURNAL OF CHROMATOGRAPHY A
www.elsevier.com/locate/chroma

Concentration dependence of lumped mass transfer coefficients Linear versus non-linear chromatography and isocratic versus gradient operation

Dorota Antos[a,*], Krzysztof Kaczmarski[a], Piątkowski Wojciech[a], Andreas Seidel-Morgenstern[b,c]

[a]*Department of Chemical Engineering, Rzeszów University of Technology, Ul. W. Pola 2, Rzeszów Pl-35-959, Poland*
[b]*Max-Planck-Institut für Dynamik komplexer technischer Systeme, D-39120 Magdeburg, Germany*
[c]*Otto-von-Guericke-Universität Magdeburg, D-39106 Magdeburg, Germany*

Abstract

The general rate model provides a reliable platform to predict elution bands in both linear and non-linear chromatography provided the required equilibrium functions and the coefficients quantifying the mass transfer in and around the particles are available. If further the variation of the equilibrium functions with changes in the mobile phase composition is known, this model is also able to predict gradient elution chromatography. Significant disadvantages of the model are the need to specify three kinetic coefficients and the amount of computing time required for the numerical solution of the underlying equations. Thus, several simplified models have been suggested lumping mass transfer resistances together. In this work the accuracy of predicting chromatographic bands based on the numerical solution of two lumped models has been analyzed. Elution profiles calculated by (a) the transport-dispersive and (b) the equilibrium-dispersive models were compared between each other and with the solution of the more detailed general rate model. In the analysis performed both linear and non-linear chromatography was considered under isocratic and gradient conditions.

Keywords: Mass transfer; Gradient elution; Adsorption; Mathematical modelling; Non-linear chromatography

1. Introduction

The application of various mathematical models for the simulation of chromatography and adsorption processes has been discussed in several excellent monographs [1–3] and a review [4]. For accurate predictions the so-called general rate model has been suggested and was frequently applied successfully [3]. This model accounts in the differential mass balance equations for axial dispersion and mass transport resistances in and around the particles. Thus, three kinetic parameters need to be specified. The solution of the equations of the general rate model further requires the application of advanced numerical techniques (as, for example, orthogonal collocation [5,6]) and significant computation times. For these reasons a number of models simplifying the transport processes have been proposed [7,8]. One of the most successful simplified models capable of describing the essential features of preparative chromatography is the so-called lumped equilibrium-dispersive model. In this model all contribu-

*Corresponding author. Tel.: +48-17-8651730; fax: +48-17-8543655.
E-mail address: dorota_antos@prz.rzeszow.pl (D. Antos).

0021-9673/03/$ – see front matter
doi:10.1016/S0021-9673(03)00948-8

tions to band broadening are quantified using an apparent axial dispersion coefficient [3]. This coefficient can be estimated from the shape of measured analytical peaks. Alternatively, in order to quantify chromatographic processes with slow mass transfer kinetics the so-called lumped transport-dispersive model has also been frequently used [9,10]. This model uses the intrinsic axial dispersion coefficient and lumps all the remaining mass transport resistances into an overall mass transport coefficient. The latter coefficient has often been determined by fitting simulated band profiles to experimental results. The solution of the two lumped models is relatively simple and does not require sophisticated numerical methods. Various finite difference methods can be utilized. To simulate elution profiles under isocratic conditions in particular the forward-backward algorithm [11] is a good tool to solve the underlying model equations. To analyze gradient elution backward-forward schemes and the Craig algorithm have been applied [12].

In linear chromatography and for isocratic elution the contributions to band broadening of different mass transfer kinetics and axial dispersion are additive and can be lumped into apparent axial dispersion or mass transport coefficients. The general rate and the equilibrium- or transport-dispersive models with lumped coefficients can generate equivalent solutions provided the applied coefficients are properly adjusted [13,14]. If non-linear conditions are considered, an agreement with the general rate model can be achieved only if concentration dependent coefficients are applied in the lumped models. The concrete dependencies required to achieve a good agreement are usually difficult to specify and have to take into account the specific courses of the adsorption isotherms. However, the application of complex functions for the apparent transport coefficients destroys the convenience of the simplified lumped models. Thus, it appears to be instructive to study the loss of accuracy connected with the usage of constant coefficients in these lumped models. In a preliminary work it has already been observed that the application of constant values leads to inaccuracies especially for low column efficiencies and strongly non-linear adsorption isotherms [15,16].

In this work the elution of single components was predicted with the lumped equilibrium-dispersive and with the lumped transport-dispersive models. As a reference the solution of the general rate model was used. The analysis has been performed for isocratic and gradient chromatography. Due to the introduced changes of the mobile phase composition during gradient elution a more pronounced effect of concentration on the values of the equivalent lumped axial dispersion and mass transport coefficients was expected than for isocratic elution.

2. Theory

To describe the models developed to simulate chromatographic separation processes it is convenient to introduce dimensionless parameters. Following widely applied conventions [17], the following dimensionless variables will be used:

$$z = \frac{x}{L}; \quad R = \frac{r}{R_p}; \quad \tau = \frac{tu}{L\varepsilon_e}; \quad C = \frac{c}{\rho_r};$$
$$C_p = \frac{c_p}{\rho_r}; \quad Q = \frac{\rho_s q}{\rho_r}; \quad Pe = \frac{uL}{D_L \varepsilon_e};$$
$$St = \frac{k_{ext} a_p L \varepsilon_e}{u}; \quad Bi = \frac{k_{ext} R_p}{D_{eff}}; \quad F_e = \frac{1-\varepsilon_e}{\varepsilon_e}; \qquad (1)$$
$$F_p = \frac{1-\varepsilon_p}{\varepsilon_p}; \quad F_t = \frac{1-\varepsilon_t}{\varepsilon_t}$$
$$\text{with } \varepsilon_t = \varepsilon_e + (1-\varepsilon_e)\varepsilon_p$$

All symbols used in Eq. (1) are explained in the Nomenclature below. The essential parameters quantifying convection, axial dispersion, external and internal mass transfer resistances are u, D_L, k_{ext} and D_{eff}. Each of the dimensionless numbers Pe, St and Bi contains two of these rate determining parameters.

2.1. Mathematical models

Below three models capable to quantify chromatographic processes will be presented. At first the most detailed general models will be introduced. Then two simple models using lumped mass transfer coefficients will be explained. More details concerning these models can be found elsewhere [3,9,16].

The general rate model consists of two partial differential mass balance equations for the changes of the concentrations in the mobile phase and of the

loading in the stationary phase. With the defined dimensionless variables this model can be expressed as:

(i) the differential mass balance equation for the mobile phase:

$$\frac{\partial C}{\partial \tau}+\frac{\partial C}{\partial z}=\frac{1}{Pe}\cdot\frac{d_p}{L}\cdot\frac{\partial^2 C}{\partial z^2}-F_e St(C-C_p|_{R=1}) \quad (2)$$

(ii) the differential mass balance equation for the stationary and the stagnant liquid phase

$$\varepsilon_p\cdot\frac{\partial C_p}{\partial \tau}+(1-\varepsilon_p)\cdot\frac{\partial Q^*}{\partial \tau}=\frac{St}{3Bi}\cdot\frac{1}{R^2}\cdot\frac{\partial}{\partial R}\cdot\left(R^2\cdot\frac{\partial C_p}{\partial R}\right) \quad (3)$$

which, for an established adsorption equilibrium within the stationary phase can be rewritten in the form:

$$(1+k_p)\cdot\frac{\partial C_p}{\partial \tau}=\frac{St}{\varepsilon_p 3Bi}\cdot\frac{1}{R^2}\cdot\frac{\partial}{\partial R}\cdot\left(R^2\cdot\frac{\partial C_p}{\partial R}\right) \quad (3a)$$

with

$$k_p=F_p\cdot\frac{dQ^*}{dC_p} \quad (3b)$$

Eqs. (2) and (3) are complemented by an equilibrium relationship coupling in Eq. (3b) the stationary and stagnant liquid phase concentrations. In this work the adsorption equilibrium was described by the single component Langmuir equation:

$$Q^*=\frac{HC_p}{1+K_r C_p}\cdot\frac{\rho_s}{\rho_r} \quad (4)$$

where for H holds: $H=q^{\infty}K_r$, with the loading capacity q^{∞} and the equilibrium constant K_r.

If in gradient elution the mobile phase composition is varied during the process due to changes of a modifier concentration C_{mod} the local equilibrium can be expressed as:

$$Q^*=\frac{H(C_{mod})C_p}{1+K_r(C_{mod})C_p}\cdot\frac{\rho_s}{\rho_r} \quad (5)$$

where the functional dependencies of the two isotherm parameters on C_{mod} have to be determined usually experimentally. In this work a dependence of H on the modifier concentration was suggested, which was found to be valid for normal-phase systems [18,19]:

$$H=(p_H C_{mod})^{-m_H} \quad (6)$$

The same type of functional dependence was also assumed for K_r, i.e.:

$$K_r=(p_{Kr}C_{mod})^{-m_{Kr}} \quad (7)$$

Thus, the quantitative description of the equilibrium loadings requires for gradients the specification of the four parameters: p_H, m_H, p_{Kr}, and m_{Kr}.

The local concentration C_{mod} can be calculated by solving Eqs. (2) and (3) for the modifier coupled with its adsorption isotherm equation. If the concentration of the modifier is much higher than the sample concentration, approximately a single component adsorption isotherm model as given with Eq. (4) can be used [20,21].

The following initial and boundary conditions complete the general rate model:

(i) initial conditions:

$$C(\tau=0,z)=C^0 \quad 0\le z\le 1 \quad (8)$$

$$C_p(\tau=0,R,z)=C^0;\quad Q^*(\tau=0,R,z)=Q^*(C^0)$$
$$0\le R\le 1,\ 0\le z\le 1 \quad (9)$$

where: $C^0=0$ for the component and $C^0=C^0_{mod}$ for the modifier.

(ii) boundary conditions for Eq. (2) and $\tau>0$:

$$C''_F(\tau,z=0)-C(\tau,z=0)=\frac{1}{Pe}\cdot\frac{\partial C(\tau,z=0)}{\partial z} \quad (10)$$

For the components a rectangular pulse injection is assumed, i.e.:

$$C''_F(\tau,z=0)=\begin{cases}C_F & \text{for } \tau\in[0,\tau_p]\\ 0 & \text{for } \tau>\tau_p\end{cases} \quad (10a)$$

For the modifier a linear concentration gradient is assumed starting after the injection is finished:

$$C'_{Fmod}(\tau,z=0)=\begin{cases}C_{Fmod} & \text{for } \tau\in[0,\tau_p]\\ C_{Fmod}+\beta(\tau-\tau_p) & \text{for } \tau_e>\tau>\tau_p\\ C_{Fmod}+\beta(\tau_e-\tau_p) & \text{for } \tau>\tau_e\end{cases} \quad (10b)$$

where β is the gradient steepness and τ_e designates the end of the gradient.

$$\left.\frac{\partial C}{\partial z}\right|_{z=1} = 0 \tag{11}$$

(iii) boundary conditions for Eq. (3) and $\tau > 0$:

$$\left.\frac{\partial C_p(\tau, z, R)}{\partial R}\right|_{R=1} = Bi(C - C_p(\tau, z, R = 1))$$

$$0 < z < 1 \tag{12}$$

$$\left.\frac{\partial C_p(\tau, z, R)}{\partial R}\right|_{R=0} = 0 \quad 0 \le z \le 1 \tag{13}$$

As mentioned above, the essential dimensionless parameters of the model quantifying band broadening effects are *Pe*, *St* and *Bi*. There are several methods available to estimate the order of magnitude of these parameters [17]. To predict Stanton and Peclet numbers, correlations recommended or used by Wilson and Geankoplis [22], Chung and Wen [23], Morbidelli et al. [7,8] and Storti et al. [24] appear to be most useful.

The numerical solution of the general rate model requires reliable methods and algorithms. To solve this type of equations the orthogonal collocation method is very suitable [5]. However, the necessity of simultaneously calculating concentration profiles in the column and within the particles leads to relatively long computation times. Thus, as an alternative approach the lumping together of several effects and the simplification of the general rate model has been suggested. The most frequently used models of this type are the equilibrium-dispersive and the transport-dispersive models which will be described below.

The equilibrium-dispersive model consist of a single differential mass balance equation for each component:

$$\frac{\partial C}{\partial \tau} + F_t \cdot \frac{\partial Q^*(C)}{\partial \tau} + \frac{\varepsilon_e}{\varepsilon_t} \cdot \frac{\partial C}{\partial z} = \frac{\varepsilon_e}{\varepsilon_t} \cdot \frac{1}{Pe_a} \cdot \frac{\partial^2 C}{\partial z^2} \tag{14}$$

If a permanent equilibrium between the two phases is assumed holds:

$$(1 + k_0) \cdot \frac{\partial C}{\partial \tau} + \frac{\varepsilon_e}{\varepsilon_t} \cdot \frac{\partial C}{\partial z} = \frac{\varepsilon_e}{\varepsilon_{tr}} \cdot \frac{1}{Pe_a} \cdot \frac{\partial^2 C}{\partial z^2} \tag{14a}$$

with

$$k_0 = F_t \cdot \frac{dQ^*(C)}{dC} \tag{14b}$$

All contributions to band broadening are lumped into an apparent dispersion coefficient and then into the apparent Peclet number $Pe_a = uL/D_a\varepsilon_e$. Thus, internal and external mass transport kinetics are accounted for indirectly and coupled with axial dispersion. Consequently, for the apparent Peclet number should hold: $Pe_a \le Pe$. Usually Pe_a is determined from the variance of a peak registered under linear conditions. Typically, the same value is then used to also describe the chromatograms under overloaded conditions [3].

The transport-dispersive model is based on a mass balance equation similar to Eq. (14). The difference is based on the fact that the loading of the solid phase is not assumed to be in equilibrium with the liquid phase concentration and the dispersion term is expressed, as in the general rate model, considering just axial dispersion:

$$\frac{\partial C}{\partial \tau} + F_t \cdot \frac{\partial Q}{\partial \tau} + \frac{\varepsilon_e}{\varepsilon_t} \cdot \frac{\partial C}{\partial z} = \frac{\varepsilon_e}{\varepsilon_t} \cdot \frac{1}{Pe} \cdot \frac{\partial^2 C}{\partial z^2} \tag{15}$$

To quantify the accumulation in the solid phase the following simple linear driving force approach is used [1,3,25,26]:

$$\frac{\partial Q}{\partial \tau} = St_m(Q^* - Q) \tag{16}$$

where

$$St_m = \frac{k_m L \varepsilon_e}{u}$$

The contributions of the external (k_{ext}) and the internal mass transport rate (k_{int}) are lumped into the coefficient k_m. The coefficient k_{int} can be related to the effective diffusion coefficient D_{eff} [24]:

$$k_{int} = \frac{5D_{eff}}{R_p} \tag{17}$$

In most applications of the model, the lumped parameters k_m or St_m are assumed to be constant and typically estimated by fitting simulated and measured peaks recorded under linear conditions.

2.2. Plate number equations

2.2.1. Moment analysis and plate numbers

In order to compare the different models used in this work it is instructive to analyze the corresponding numbers of theoretical plates. Based on classical residence time analysis plate numbers can be determined from the first absolute moment, μ_1, and the second central moment, μ_2' (which corresponds to the variance σ^2) of a calculated band profile. These moments are defined as follows:

$$\mu_1 = \frac{\int_0^\infty tC(t)\mathrm{d}t}{\int_0^\infty C(t)\mathrm{d}t} \tag{18}$$

$$\mu_2' = \sigma^2 = \frac{\int_0^\infty (t-\mu_1)^2 C(t)\mathrm{d}t}{\int_0^\infty C(t)\mathrm{d}t} \tag{19}$$

The corresponding number of theoretical plates, N^{eff}, is:

$$N^{\mathrm{eff}} = \frac{\mu_1^2}{\sigma^2} \tag{20}$$

Thus a column of length L has the following height equivalent to a theoretical plate, *HETP*:

$$HETP = L/N^{\mathrm{eff}} = \frac{L\sigma^2}{\mu_1^2} \tag{21}$$

To achieve a close agreement between predictions of band profiles using different models it is necessary that at least the corresponding theoretical moments defined in Eqs. (18) and (19) and thus the plate numbers N^{eff} are identical (or very close to each other). Perfect agreement can be expected of course only if the higher moments, not considered here, are also identical.

2.2.2. Plate number equations: isocratic mode

2.2.2.1. General rate model

(i) Linear isotherms. For linear conditions there exist well know treatments quantifying dispersion phenomena in chromatographic columns [2,14,27–29]; in the corresponding plate number and plate height equations all non-equilibrium effects are additive. For the first absolute and second central moments corresponding to the general rate model holds:

$$\mu_1 = \frac{L}{(u/\varepsilon_\mathrm{e})}\cdot(1+k_1) \tag{22}$$

$$\sigma^2 = \mu_2' = \frac{2L}{(u/\varepsilon_\mathrm{e})}\cdot(\delta_{\mathrm{ax}} + \delta_{\mathrm{ext}} + \delta_{\mathrm{in}}) \tag{23}$$

where: $\delta_{\mathrm{ax}}, \delta_{\mathrm{ext}}, \delta_{\mathrm{in}}$ are contributions of axial dispersion, external and internal mass transport resistances to band broadening. For these contributions holds:

$$\delta_{\mathrm{ax}} = \frac{D_\mathrm{L}}{(u/\varepsilon_\mathrm{e})^2}\cdot(1+k_1)^2 = \frac{1}{Pe}\cdot\frac{L}{(u/\varepsilon_\mathrm{e})}\cdot(1+k_1)^2 \tag{24}$$

$$\delta_{\mathrm{ext}} = \frac{d_\mathrm{p}}{6k_{\mathrm{ext}}F_\mathrm{e}}\cdot k_1^2 = \frac{1}{StF_\mathrm{e}}\cdot\frac{L}{(u/\varepsilon_\mathrm{e})}\cdot k_1^2 \tag{25}$$

$$\delta_{\mathrm{in}} = \frac{d_\mathrm{p}^2}{60D_{\mathrm{eff}}F_\mathrm{e}}\cdot k_1^2 = \frac{Bi}{5StF_\mathrm{e}}\cdot\frac{L}{(u/\varepsilon_\mathrm{e})} \tag{26}$$

The constant k_1 is expressed as:

$$k_1 = F_\mathrm{e}\cdot\left(\varepsilon_\mathrm{p} + (1-\varepsilon_\mathrm{p})H\cdot\frac{\rho_\mathrm{s}}{\rho_\mathrm{r}}\right) = F_\mathrm{e}\varepsilon_\mathrm{p}\cdot\left(1 + F_\mathrm{p}H\cdot\frac{\rho_\mathrm{s}}{\rho_\mathrm{r}}\right) \tag{27}$$

where $H\cdot\rho_\mathrm{s}/\rho_\mathrm{r}$ is the isotherm slope, i.e.:

$$H\cdot\frac{\rho_\mathrm{s}}{\rho_\mathrm{r}} = \frac{\mathrm{d}Q^*}{\mathrm{d}C} \tag{27a}$$

Substituting Eqs. (22–26) into Eq. (20) the following equation can be derived to specify the plate number of the general rate model, N_{grm}:

$$\frac{1}{N_{\mathrm{grm}}} = \frac{2}{Pe} + 2\cdot\left(\frac{k_1}{1+k_1}\right)^2\cdot\left[\frac{Bi}{5F_\mathrm{e}St} + \frac{1}{F_\mathrm{e}St}\right] = \frac{2}{Pe} + 2\cdot\left(\frac{k_1}{1+k_1}\right)^2\cdot\frac{1}{F_\mathrm{e}St_{\mathrm{ov}}} \tag{28}$$

In the above for the overall Stanton number St_{ov} holds:

$$St_{ov} = \frac{St}{1 + Bi/5} = \frac{k_{ov} a_p L \varepsilon_e}{u} \quad (29)$$

Typically, in chromatographic processes the contribution of external mass transfer resistances is small [30]. Then the term $(1/F_e St)$ can be neglected in Eq. (28) simplifying Eq. (29):

$$St_{ov} = \frac{5St}{Bi} \quad (29a)$$

Then the ratio St/Bi can be treated as an adjustable parameter that can be determined by matching experimental and simulated peaks under linear conditions. Since the determining of F_e is usually difficult this parameter can be further lumped together with the ratio St/Bi and $F_e St/Bi$ can be determined from experiments.

For the overall mass transport coefficient k_{ov} in Eq. (29) holds:

$$k_{ov} = \left(\frac{1}{k_{ext}} + \frac{1}{k_{int}} \right)^{-1} \quad (30)$$

(ii) Non-linear isotherms. The analysis of variances or plate numbers characterizing a chromatographic peak or a breakthrough curve becomes more complex if the adsorption isotherms are non-linear. Now these quantities do not depend only on the Henry constant and the mass transfer parameters but also on the concentration range covered. As shown by Rhee and Amundson [31] there is a simplified analysis possible for self-sharpening fronts that are characterized by very rapid concentration changes. Such fronts establish in case of favorable isotherms and for sufficient column lengths. Under these conditions the contributions of axial dispersion and external and internal mass transport resistances are additive even under non-linear conditions. To estimate the variance of such shock layers the equations presented above can be used, provided k_1 in Eq. (27) is calculated differently based on the isotherm chord [32], i.e.:

$$k_1 = F_e \cdot \left(\varepsilon_p + (1 - \varepsilon_p) \cdot \frac{Q^*(C_s|_+) - Q^*(C_s|_-)}{(C_s|_+ - C_s|_-)} \right) \quad (31)$$

Above the $C_s|_-$, $C_s|_+$ designate the concentrations before and after the concentration jump and k_1 is related to the corresponding retention time of the front. Thus, as in linear chromatography, the variance of a certain shock front can be described with a single constant plate number. Although self-sharpening fronts begin to form frequently in preparative chromatography, the column lengths applied are not always sufficiently large to allow for the complete formation of the constant pattern behavior.

In contrast to self-sharpening fronts, dispersed fronts also occur due to isotherm non-linearities. These dispersed fronts are characterized by a thermodynamically determined retention time distribution. The corresponding concentration dependent k_1 values must be related to the local isotherm slope. They vary with the local concentration according to:

$$k_1(C) = F_e \cdot \left(\varepsilon_p + (1 - \varepsilon_p) \cdot \frac{dQ^*}{dC} \right) \quad (32)$$

with

$$\frac{dQ^*}{dC} = \frac{H}{(1 + K_r C)^2} \cdot \frac{\rho_s}{\rho_r} \quad (32a)$$

These concentration dependent k_1 values instead of Eq. (27) are capable of describing the variances of responses curves belonging to small pulses injected on certain concentration levels.

Overloaded peaks under non-linear conditions are typically characterized by the presence of compressed and dispersed fronts. A general prediction of the variance of such elution profiles also considering mass transfer resistances is only possible by numerically solving the equation of a column model. To find conditions under which the results of different column models converge as closely as possible requires tedious numerical calculations. Below instead the use of just Eqs. (31) and (32) will be attempted, to match as closely as possible the predictions of the three models considered in this paper. For this it remains to specify the plate height equations for the equilibrium-dispersive and the transport dispersive models.

2.2.2.2. Equilibrium-dispersive model

In the equilibrium-dispersive model all contributions to band broadening are lumped into the apparent Peclet number, Pe_a. For linear condition the plate number of the equilibrium-dispersive model, N_{edm}^{eff},

can be simply calculated from this quantity according to:

$$\frac{1}{N_{\mathrm{edm}}^{\mathrm{eff}}} = \frac{\sigma^2}{\mu_1^2} = \frac{\varepsilon_e}{\varepsilon_t} \cdot \frac{2}{Pe_a} \tag{33}$$

Obviously to match the solutions of the equilibrium-dispersive and the general rate models should hold $N_{\mathrm{grm}} = N_{\mathrm{edm}}^{\mathrm{eff}}$, i.e.

$$\frac{1}{Pe_a} = \frac{1}{Pe} + \left(\frac{k_1}{1+k_1}\right)^2 \cdot \frac{1}{F_e St_{ov}} \tag{34}$$

Thus, in order to use successfully the simpler equilibrium-dispersive model, equivalent apparent Peclet numbers have to be applied. To determine such numbers the values for Pe, k_1, F_e and St_{ov} have to be provided.

If concentration dependent k_1 values are used [Eq. (32)], the apparent Peclet number will also be concentration dependent, i.e. $Pe_a = Pe_a(C)$. For typical chromatographic conditions usually the term $1/Pe$ in Eq. (34) is small compared to the contributions of the two mass transport resistances quantified by St_{ov}.

2.2.2.3. Transport-dispersive model

Based on an analytical solution of the transport-dispersive model for linear isotherms, Lapidus and Amundson [13] quantified band broadening effects. The corresponding plate height equation of this model can be written in the following dimensionless form [15,16]:

$$\frac{1}{N_{\mathrm{tdm}}^{\mathrm{eff}}} = \frac{2}{Pe} + 2 \cdot \left(\frac{k_0}{1+k_0}\right)^2 \cdot \frac{\varepsilon_e}{\varepsilon_t k_0 St_m} \tag{35}$$

where k_0 is the retention factor, which for linear conditions is expressed as:

$$k_0 = F_t H \cdot \frac{\rho_s}{\rho_r} \tag{36}$$

Matching N_{grm} and $N_{\mathrm{tdm}}^{\mathrm{eff}}$ [i.e. Eqs. (28) and (35)], one obtains:

$$\frac{1}{St_m} = k_0 \cdot \frac{\left(\frac{k_1}{1+k_1}\right)^2}{\left(\frac{k_0}{1+k_0}\right)^2} \cdot \frac{\varepsilon_t}{\varepsilon_e F_e St_{ov}} \tag{37}$$

After rearranging St_m can be expressed as:

$$St_m = \frac{k_0}{(1+k_0)^2} \cdot \left(\frac{1}{k_1}+1\right)^2 \cdot \frac{\varepsilon_e F_e St_{ov}}{\varepsilon_t} \tag{38}$$

As for the k_1 above [Eqs. (31) and (32)] for shock layers formed under non-linear conditions can be assumed:

$$k_0 = F_t \cdot \frac{Q^*(C_s|_+) - Q^*(C_s|_-)}{(C_s|_+ - C_s|_-)} \tag{39}$$

Analogously to calculate k_0 for dispersed fronts the local slope of the isotherm can be applied:

$$k_0 = F_t \cdot \frac{H}{(1+K_r C)^2} \cdot \frac{\rho_s}{\rho_r} \tag{40}$$

The second moments corresponding to the transport-dispersive model become equivalent to that corresponding to the general rate model if the lumped Stanton number, St_m, fulfills Eq. (37). To realize this matching the required parameters: k_0, k_1, ε_e, ε_t, F_e and St_{ov} have to be provided. If concentration dependent k_0 and k_1 values are used also the lumped Stanton number will be concentration dependent, i.e. $St_m = St_m(C)$.

2.2.3. Plate number equations: gradient elution

In order to simulate elution processes under solvent gradient conditions an additional differential mass balance equation for the modifier has to be solved. The isotherm parameters of a certain solute are not constant but depend on the local modifier concentration. This leads to the fact that for gradient elution the two coefficients k_0 and k_1 [(Eqs. (31), (32), (39), (40)] also vary with changes of the mobile phase composition. Thus, the concentration dependencies of the apparent Pe_a number and the lumped St_m number are more complex than for isocratic conditions. Again a simplified situation is encountered if the isotherms of the solutes remain linear for all solvent compositions.

2.2.3.1. Linear isotherm

For linear conditions the local values of the coefficients k_0; k_1 can be simply expressed as:

$$k_0 = F_t \cdot \left(H(C_{\mathrm{mod}}) \cdot \frac{\rho_s}{\rho_r}\right) \tag{41}$$

$$k_1 = F_e \cdot \left[\varepsilon_p + (1-\varepsilon_p) H(C_{mod}) \cdot \frac{\rho_s}{\rho_r} \right] \quad (42)$$

where again $H(C_{mod}) \cdot \rho_s/\rho_r$ is the initial isotherm slope, i.e. $H(C_{mod}) \cdot \rho_s/\rho_r = (dQ^*/dC)|_{C\to 0}$ for the concentration of the modifier at C_m. The local values of H can be calculated from the local modifier concentration, provided the mutual dependence is known.

2.2.3.2. Non-linear isotherm

If the isotherms are non-linear the situation is very complex. The simplest case is again the description of the migration of shock layers, which can be also formed under gradient conditions. For such fronts the values of k_0 and k_1 depend in the following manner on the local modifier concentrations:

$$k_0 = F_t \cdot \left(\frac{Q^*(C_s|_+, C_{mod}|_+) - Q^*(C_s|_-, C_{mod}|_-)}{(C_s|_+ - C_s|_-)} \right) \quad (43)$$

$$k_1 = F_e \varepsilon_p \left(1 + \frac{(1-\varepsilon_p)}{\varepsilon_p} \cdot \frac{Q^*(C_s|_+, C_{mod}|_+) - Q^*(C_s|_-, C_{mod}|_-)}{(C_s|_+ - C_s|_-)} \right) \quad (44)$$

where $C_s|_-, C_s|_+, C_{mod}|_-, C_{mod}|_+$ are related to the concentrations of the plateaus before and after the concentrations jump. This analysis is valid provided that competition between sample and modifier can be neglected. This is often the case in gradient chromatography, wherein concentration of the modifier in the mobile phase is markedly higher than that of the sample, hence adsorption of the sample does not perturb adsorption equilibrium of the modifier. Otherwise competitive isotherm equations must be applied. The general difference from the isocratic situation [Eqs. (31) and (39)] is the fact that the speed of the fronts is influenced by the modifier concentration.

For simulating dispersed fronts concentration dependent parameters k_0 and k_1 can be estimated by again replacing the isotherm chord by the local isotherm slope, i.e.:

$$k_0 = F_t \cdot \left\{ \frac{H(C_{mod})}{[1 + K_r(C_{mod})C]^2} \right\} \quad (45)$$

$$k_1 = F_e \cdot \left\{ \varepsilon_p + (1-\varepsilon_p) \cdot \frac{H(C_{mod})}{[1 + K_r(C_{mod})C]^2} \right\} \quad (46)$$

In order to determine these values the local modifier concentration profile $C_{mod}(\tau, z)$ has to be known.

From the above it is evident that under gradient conditions a close matching between the results of the general rate model and the results of the two lumped models is more difficult. To reach this goal it is obviously required to include in the lumped coefficients in addition to the local concentration of the solutes also the local mobile phase composition.

3. Numerical methods

The three models introduced above were used for simulating band profiles for different isocratic and gradient conditions. Systems of ordinal differential equations were obtained after discretizing the partial differential equations using the orthogonal collocation on finite elements method [5]. These ordinary differential equations were integrated using the VODE procedure [33] for relative and absolute error of 10^{-6}. This procedure automatically chooses the appropriate time increment to fulfill the specified error conditions. In each calculation the number of internal collocation points [5] was equal to 3 for the column and equal to 4 for the particles (for solving the equations of the general rate model). The number of subdomains chosen guaranteed that no visible oscillation in band profile calculations occurred.

In order to simulate the gradient process the adequate differential mass balance equations [Eqs. (2) and (3) for the general rate model, Eq. (14) for the equilibrium-dispersive model and Eqs. (15) and (16) for the transport-dispersive model] were solved together for the sample component and the modifier. A detailed description of the procedure applied can be found elsewhere [20].

4. Results and discussion

4.1. Model parameters

The model parameters used in the simulation study

Table 1
Model parameters used in the simulation study

ε_e	ε_p	ρ_s (kg/m^3)	H (−)	K_r (m^3/kmol)	c_F	Pe	$N^{eff}\varepsilon_e/\varepsilon_t$	St/Bi
0.33	0.52	1960	8	4	0.1–0.6	1000	275 or 44	100 or 5

are summarized in Table 1. The value for the reference density was assumed to be $\rho_r = 1$. In this case the dimensionless concentrations in the mobile and stagnant liquid phases, C and C_p, correspond exactly to c and c_p. As indicated by the product of K_r and the maximal feed concentrations c_F (4*0.6 = 2.4) the process was investigated up to strongly non-linear conditions. The simulations using the general rate model were performed with $Pe = 1000$. By varying the ratio St/Bi in two steps a relatively low and a relatively high column efficiency could by analyzed. For different conditions, as a reference solutions of the general rate model were calculated. The lumped equilibrium-dispersive and the transport-dispersive models were solved with apparent Pe_a [Eq. (34)] and St_m [Eq. (37)] numbers as described above. In order to take into account concentration effects, the required values for k_1 and k_0 could be calculated in different ways. The following three options were considered:

(1) Eqs. (27) and (36) [or Eqs. (41) and (42) for gradients], valid for linear conditions

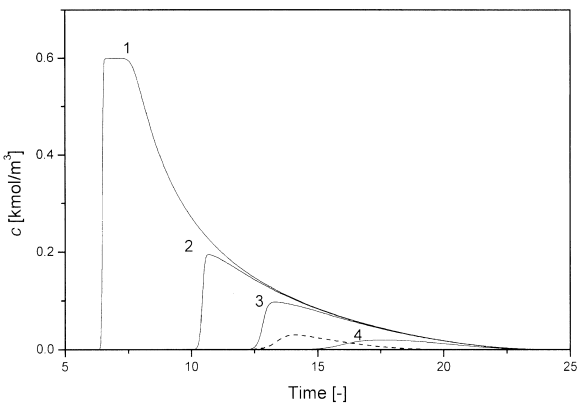

Fig. 1. Reference profiles calculated by general rate model with $St/Bi = 100$, $Pe = 1000$. Curve 1, $c_F = 0.6$, $\tau_p = 4.5$ [−] (the injection volume is 225% of the column dead volume); curve 2, the same as curve 1 but $c_F = 0.2$; curve 3, the same as curve 1 but $c_F = 0.1$; curve 4, the same as curve 1 but $c_F = 0.02$; dashed line, the same as curve 1 but $\tau_p = 0.15$ [−] and injection volume is 7.5% of the column dead volume.

(2) Eqs. (31) and (39) [or Eqs. (43) and (44) for gradients], applicable for shock fronts
(3) Eqs. (32) and (40) [or Eqs. (45) and (46) for gradients], applicable for dispersed fronts

In extensive preliminary calculations, not illustrated below, it was confirmed that for linear conditions (i.e. for $K_r = 0$) the lumped models are indeed equivalent to the general rate model provided the applied Pe_a and St_m numbers are in agreement with Eqs. (27) and (36) [or (41) and (42) for gradients].

4.2. Isocratic mode

To cover typical non-linear situations a series of injections of identical sample volumes with different feed concentrations (reaching the non-linear range of the isotherm) was simulated using the general rate model. Fig. 1 illustrates for a relatively high column efficiency ($Pe = 1000$, $St/Bi = 100$) the well known effects of formation of sharp and dispersed fronts and the erosion of the concentration plateau corresponding to the feed concentration if small concentrations are injected. In profile 1 the shock layer and the dispersed front are still separated by a plateau corresponding to $c_F = 0.6$. For decreased feed concentrations the plateau disappears and the sharp and dispersed fronts merge (profiles 2 and 3). If the concentrations are sufficiently low the sharp fronts also disperse (profile 4). The dashed profile in Fig. 1 illustrates the effect of changing the injection volume for maintained sample amount compared to profile 4. Further reference profiles were calculated but for a relatively low efficiency ($St/Bi = 5$).

Before analyzing the results obtained with the two lumped models it is instructive to evaluate the concentration effects on the corresponding k_1, k_0, and Pe_a, St_m values for the range studied (i.e for $C^{min} = 0$ and $C^{max} = 0.6$). The concentration dependence of the apparent Pe_a number [Eq. (34)] applied in the equilibrium-dispersive model is related to $[(k_1 + 1)/k_1]^2$. For the reference parameters used here and applying Eq. (32), this term is 1.12 for C^{min} and

2 for C^{max} [Eq. (32)]. For the chord connecting C^{min} and C^{max} results an intermediate value of 1.4 is found [Eq. (31)]. The concentration dependence of the St_m number is according to Eq. (37) related to the term $k_0\,((1+k_1)^2/(1+k_0))^2$. Applying again Eqs. (32) and (40) yields for this term 0.12 (for $C^{min}=0$) and 0.48 (for C^{max}). For the corresponding chord [Eqs. (31) and (39)] a value of 0.30 is obtained. Obviously, there is a stronger concentration effect on the lumped St_m number than on the apparent Pe_a number.

In the following the accuracy of predicting the calculated reference profiles with the two lumped models will be analyzed for two different levels of column efficiency.

4.2.1. Relatively high column efficiency

At first simulations were carried out for $Pe=1000$ and $St/Bi=100$, i.e. for a relatively efficient column. Breakthrough curves corresponding to profile 1 in Fig. 1 were calculated with the two lumped models using the three possible options available to estimate the k_1 and k_0 values. For both lumped models these options gave similar results. In Fig. 2 are depicted (together with the breakthrough curve which was calculated with the general rate model) the results of the two lumped models using Eqs. (27) and (36) based on the steepest (initial) slope and corresponding to $St_m=19.6$ and $Pe_a=550$ (or $N^{eff}\varepsilon_e/\varepsilon_t=275$). It is evident that the accuracy of predictions with both lumped models using constant Pe_a and St_m numbers is relatively good compared to the solution of the general rate model. Eqs. (27) and (36), i.e. the constant initial isotherm slope, were also used to simulate with the two lumped models the rather diluted elution profile corresponding to the dashed line in Fig. 1 ($c^{Max}K_r=0.4<1$). The results shown in Fig. 3 reveal a similar agreement between the three models as for the breakthrough curves shown in Fig. 2.

These and further results indicate that for the description of band profiles for relatively high column efficiencies (theoretical plate numbers larger than $N^{eff}\varepsilon_e/\varepsilon_t>200$) constant lumped coefficients taken from the initial isotherm slope might be successfully applied.

4.2.2. Relatively low column efficiency

For lower column efficiencies ($Pe=1000$ and $St/Bi=5$ corresponding to $N^{eff}\varepsilon_t/\varepsilon_e=44$) and nonlinear conditions the differences of the predictions of the three models were found to be more significant than for higher efficiencies.

At first the breakthrough curve from Fig. 1 (profile 1) was recalculated for the lower efficiency with all models. In the calculation with the two lumped models k_1 and k_0 were determined (a) using again Eqs. (27) and (36) (exploiting only the initial

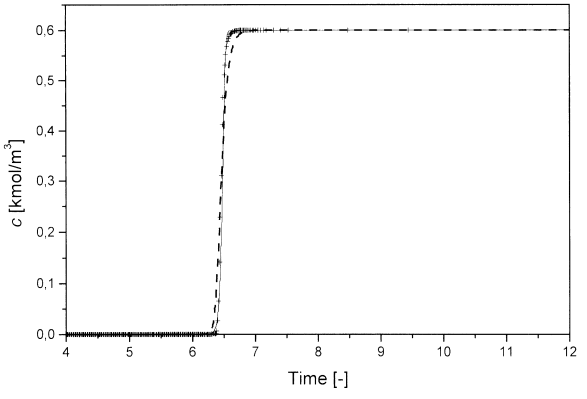

Fig. 2. Comparing predictions of a breakthrough curve for a relatively high efficiency ($St/Bi=100$, $Pe=1000$). Parameters correspond to curve 1 in Fig. 1; solid line, general rate model; crosses, equilibrium-dispersive model, $N^{eff}\varepsilon_e/\varepsilon_t=275$, k_1 Eq. (27); dashed line, transport-dispersive model, $St_m=19.6$, k_1 and k_0 from Eqs. (27) and (36).

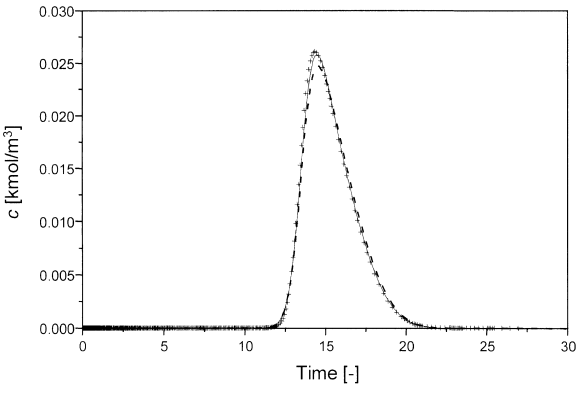

Fig. 3. Comparing predictions of elution profiles for a relatively high efficiency ($St/Bi=100$, $Pe=1000$). Parameters correspond to the dashed line in Fig. 1. Lines and symbols correspond to Fig. 2. k_1 and k_0 from Eqs. (27) and (36).

isotherm slope), (b) using Eqs. (31) and (39) (exploiting the isotherm chord) for simulating the sharpened front and (c) using Eqs. (32) and (40) (exploiting the concentration dependent local slopes) for simulating the dispersed front. The accuracy of simulations using the equilibrium-dispersive model was already acceptable with a constant Pe_a number according to Eqs. (27) and (36), i.e. influence of the isotherm non-linearity on the prediction quality was negligible. The most pronounced inaccuracies were exhibited by simulations of the transport-dispersive model with a constant St_m number [Eqs. (27) and (36)]. The accuracy of predicting with this model the sharpened and the dispersed front was significantly improved when the non-linearity of the isotherm was accounted for by the corresponding Eqs. (31) and (39) or (32) and (40).

Fig. 5 shows the concentration dependence of the two lumped parameters Pe_a and St_m corresponding to the dispersed fronts given in Fig. 4 and calculated with Eqs. (32) and (40). Obviously the change in the size of the parameters is much more pronounced for the parameter of the transport-dispersive model, St_m. Averaging this latter value appears to be critical and had already been found to cause inaccurate results in the description of breakthrough curves of bovine serum albumin (BSA) in anion-exchange chromatography [16].

Subsequently chromatographic band profiles were calculated for an injected amount not sufficient to reach at the column outlet the injection concentration

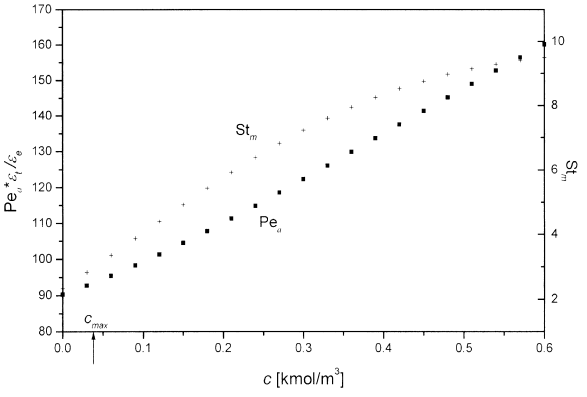

Fig. 5. Concentration dependence of St_m and Pe_a numbers in simulations of dispersed fronts in isocratic mode corresponding to the dispersed front in Fig. 4 according to Eqs. (32) and (40).

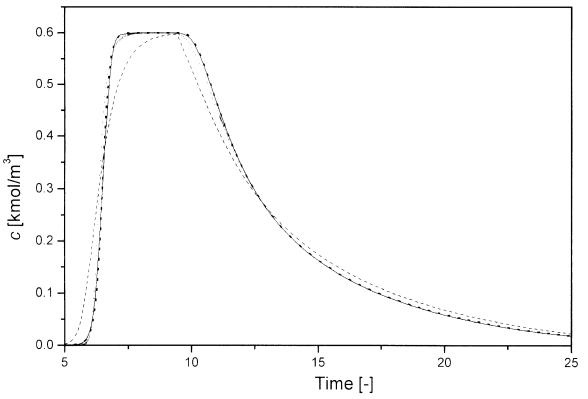

Fig. 4. Influence of a model type on the accuracy of the band broadening prediction for a relatively low efficiency. Model parameters as in Table 1 and for curve 1 in Fig. 1. Solid line, band profiles calculated with the general rate model; dashed line, transport-dispersive model, $St_m = 2.2$ [k_1, k_0 from Eqs. (27) and (36)]; crosses, equilibrium-dispersive model, $N^{eff}\varepsilon_e/\varepsilon_t = 44$ [k_1 from Eq. (27)]; dotted line, transport-dispersive model with the non-linear correction [k_1, k_0 from Eqs. (31) and (39) for the sharpened front and from Eqs. (32) and (40) for the dispersed front].

(compare curves 2–4 in Fig. 1). As could be expected, the application of Eqs. (31) and (39) in combination with the feed concentration delivered such constant k_1 and k_0 that led to profiles significantly too sharp. Thus, in Figs, 6 and 7 are shown only the results for the cases where k_1 and k_0 were calculated using (a) Eqs. (27) and (36) (constant isotherm slope) and (b) Eqs. (32) and (40) (local isotherm slope). The same trend as in Fig. 4 was

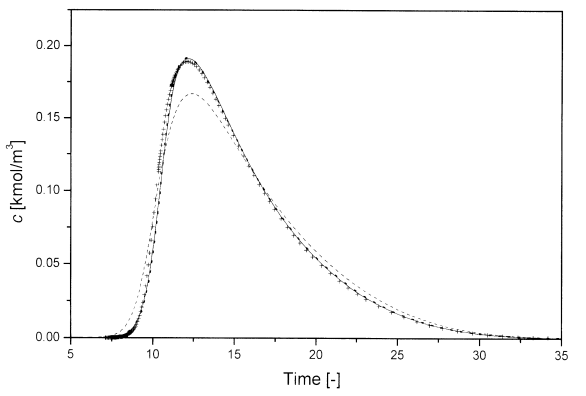

Fig. 6. Influence of a model type on the accuracy of the band broadening prediction for a relatively low efficiency. Lines as in Fig. 4, model parameters as in Table 1 and for curve 2 in Fig. 1.

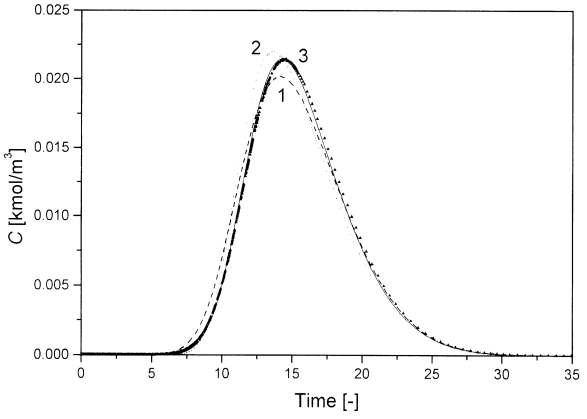

Fig. 7. Influence of a model type on the accuracy of the band broadening prediction for a relatively low efficiency. Model parameters as in Table 1 and for dashed line in Fig. 1. Solid line, band profiles calculated with the general rate model; 1, transport-dispersive model, $St_m = 2.2$ [k_1, k_0 from Eqs. (27) and (36)]; 2, equilibrium-dispersive model, $N^{eff}\varepsilon_e/\varepsilon_t = 44$ [k_1 from Eq. (27)]; 3, transport-dispersive model with the non-linear correction [k_1, k_0 from Eqs. (31) and (39) for the sharpened front and from Eqs. (32) and (40) for the dispersed front].

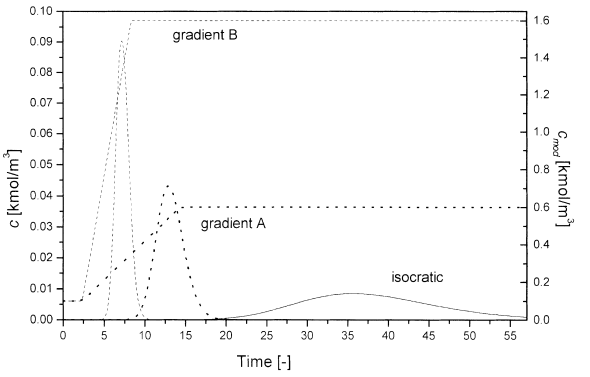

Fig. 8. Influence of gradient steepness on the chromatographic profiles (calculations with the general rate model). Gradient steepness: the change of $C_{Fmod} = 0.1$ to $C_{Fmod} = 0.6$ in $\tau_p = 12$ [−] (gradient A) and $C_{Fmod} = 0.1$ to $C_{Fmod} = 1.6$ in $\tau_p = 6$ [−] (gradient B). The parameters of Eqs. (6) and (7) are: $m_H = 1$, $m_{Kr} = 1$, $p_H = 0.5$, $p_{Kr} = 2$.

observed, i.e. the simulations with the transport-dispersive model were the most inaccurate (Fig. 7). The differences between simulations of all models vanish the more the peaks are diluted (from Fig. 6 to Fig. 7).

4.3. Gradient elution

Similar calculations as described above were performed for the gradient elution. Linear gradients in accordance with Eq. (10a) were considered. For the sake of simplicity the modifier was assumed to be not retained, which is typical if the column is initially equilibrated by the modifier, i.e. $H_{mod} \cong 0$, $K_{rmod} \cong 0$ were used for the simulations. The well-known effect of gradient steepness on the chromatographic band profiles is illustrated in Fig. 8. The gradient profiles of the modifier for two different gradient steepnesses are superimposed to the band profiles of the sample component. The process parameters are summarized in Table 2.

In the simulations of gradient elution only chromatographic peaks not reaching at the column outlet the feed concentration were considered. As discussed above under gradient conditions the lumped dispersion and mass transport coefficients also now depend on the mobile phase composition. In gradient elution modifier concentration changes are usually imposed in order to create severe changes in the isotherm slopes or chords. This leads to pronounced changes in the values of the appropriate lumped transport coefficients. Thus, the lumped coefficient determined for initial (the start of gradient) and final (the end of gradient) concentration levels can be markedly different. This ‘‘modifier’’ or ‘‘retention’’ dependence can be much more pronounced compared to the concentration dependence connected with the isotherm non-linearity discussed above. In systematic calculations for the parameter used in this study the values of the lumped Stanton number were found to be more sensitive to the mobile phase composition than those of the apparent Peclet number. Typical St_m and Pe_a numbers calculated for the initial and final modifier concentration for two gradient steepnesses are summarized in Table 2.

The simulations of chromatographic profiles were performed for both lumped models at:

(1) constant initial and final St_m and Pe_a numbers related to the slope of the linear isotherm at initial or final saturation level, respectively. For calculating initial and final H values the functional dependency $H(C_{mod})$ given by Eq. (6) was used.

(2) local non-constant values of St_m and Pe_a numbers corresponding to the local isotherm slope

Table 2
Model parameters used in the gradient elution simulation study

	Gradient steepness	St_m [a]	St_m [b]	Pe_a [a]	Pe_a [b]	$\varepsilon_t/\varepsilon_e N$	Modifier isotherm
Gradient A	C_{mod} change 0.1–0.6 (kmol/m^3) in 400 s	1.0	4.7	82	101	50.5	$H=0$, $K_{rmod}=0$
Gradient B	C_{mod} change 0.1–1.6 (kmol/m^3) in 200 s	1.0	5.95	82	129	64	$H=0$, $K_{rmod}=0$

[a] Calculated at the constant isotherm slope related to the initial ($C_{mod}=0.1$) saturation level.
[b] Calculated at the constant isotherm slope related to the final ($C_{mod}=0.6$ or 1.6, gradients A or B) saturation level.

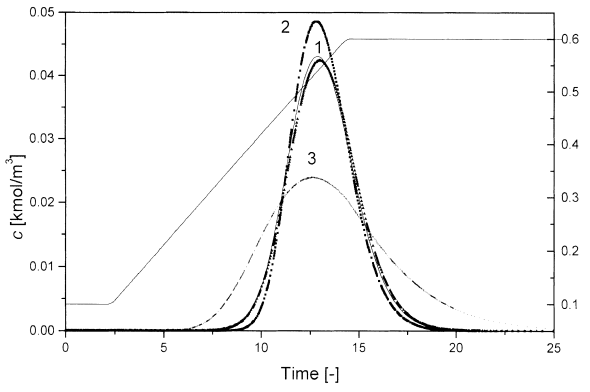

Fig. 9. Comparison between simulations with the general rate and the transport-dispersive model in gradient elution. $c_F=0.6$, $\tau_p=0.3$ [−]. Gradient A. Solid line, the solution with the general rate model; symbol 1, local values of St_m number related to local isotherm parameters [Eqs. (45) and (46)]; symbols 2 and 3, final and initial constant St_m numbers (Table 2, gradient A).

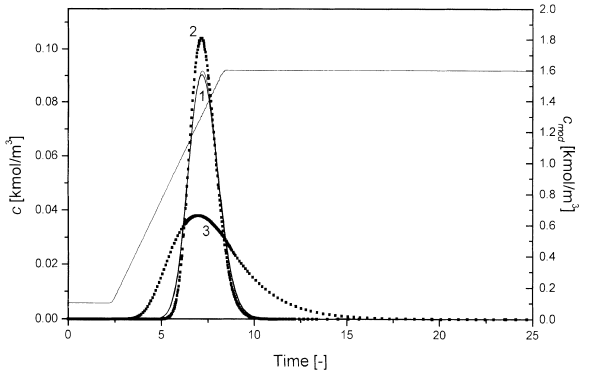

Fig. 10. Comparison between simulations with the general rate and transport-dispersive model in gradient elution. Gradient B (Table 2, gradient B). Lines as in Fig. 9.

according to Eqs. (45) and (46). The appropriate actual isotherm parameters $H(C_{mod})$ and $K_r(C_{mod})$ were determined from the relationship given by Eqs. (6) and (7).

4.3.1. Transport-dispersive model

In Figs. 9 and 10 results of simulations for the transport-dispersive model for two different gradient steepnesses (gradients A and B in Table 2) are shown.

It is apparent that assumption of constant mass transport coefficients leads to significant errors, which become more pronounced for strong gradient steepnesses. The St_m number depends strongly on the local values of the k_0, k_1 coefficients. St_m increases distinctly with increasing modifier concentration and after achieving a maximum drops slowly (Fig. 13). This phenomenon can be explained by the effect of the variation of the Henry constant (H) on the coefficients k_0, k_1. For higher H the contribution of the term $(1/k_1+1)^2$ in Eq. (38) prevails and St_m increases with decreasing H. In the range of low H ($H<1$) its influence on k_1 vanishes while the term $k_0/(1+k_0)^2$ decreases continuously [compare Eqs. (38), (41) and (42)]. For illustration the values of the St_m calculated for the initial and final saturation level related to the start and the end of the gradient program are summarized Table 2.

4.3.2. Equilibrium-dispersive model

The same analysis was performed for the equilibrium-dispersive model. In gradient elution the equilibrium-dispersive model with constant axial dispersion coefficient also gives better results compared to those generated by the corresponding trans-

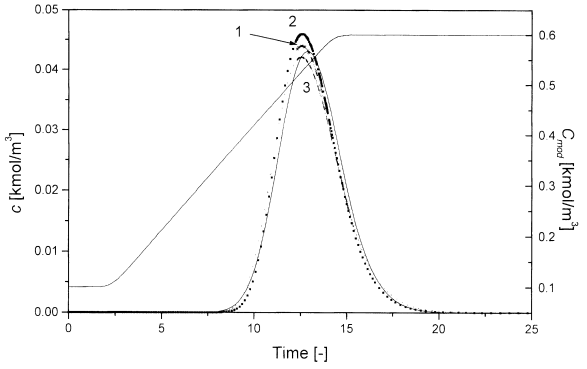

Fig. 11. Comparison between simulations with the general rate and the equilibrium-dispersive model in gradient elution. Gradient A. Solid line, solution with the general rate model; symbol 1, local values of Pe_a number [Eq. (46)]; symbols 2 and 3, final and initial Pe_a numbers (Table 2, gradient A).

port-dispersive model. However, the influence of retention dependence can be pronounced for strong gradients, for which the sample components are weakly retained or non-retained at the end of gradient (compare Figs. 11 and 12). The variation of Pe_a is illustrated in Fig. 13. The values of the Pe_a number related to the initial and final saturation level are shown in Table 2.

It is evident (in Fig. 13) that the influence of the modifier concentration changes on the apparent Peclet number is smaller than on the lumped Stanton number. The former reaches an asymptotic value whereas the latter varies in the whole range of modifier concentrations or retention factors.

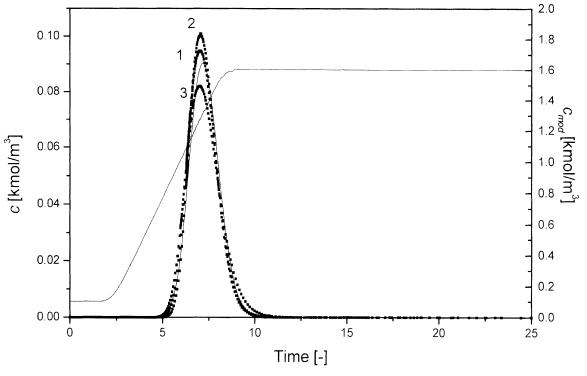

Fig. 12. Comparison between simulations with the general rate and the equilibrium-dispersive models in gradient elution. Gradient B. Lines as in Fig. 11.

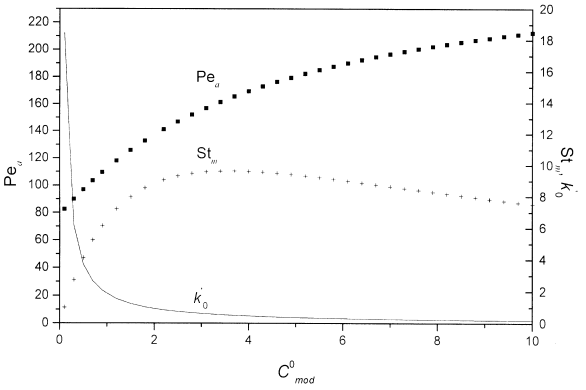

Fig. 13. Variation of the apparent Peclet number (corresponding to $N^{eff}\varepsilon_e/\varepsilon_t = Pe_a/2$), the lumped Stanton number and the retention factor with the modifier concentration.

5. Conclusion

The influence of concentration and retention dependences of apparent dispersion and mass transport coefficients on the accuracy of band profile prediction using the lumped equilibrium-dispersive and transport-dispersive models has been discussed. The simulations of both the models were compared between each other and with the general rate model.

For isocratic elution the assumption of constant lumped coefficients in the commonly used equilibrium and transport-dispersive models leads to inaccuracies in the prediction of band broadening in low efficiency systems. However, due to the typically strong peak dilution in chromatographic processes, enhanced by kinetic effects, the concentration dependence of the lumped transport coefficients can be often neglected. Both the lumped models studied can be safely used in a broad range of column efficiencies. Errors in predictions using constant parameters are most probable in simulating bands undergoing severe concentration changes. Thus, errors can be expected in particular in simulations of chromatography processes where concentrating effects are involved as in displacement chromatography. Due to the character of the concentration dependencies the lumped mass transport coefficient appears to be more sensitive to concentration changes than the apparent axial dispersion coefficient. Thus, the lumped equilibrium-dispersive model with constant apparent axial dispersion coefficient generated in our study

more accurate results in simulating band profiles compared to the lumped transport-dispersive model.

For gradient elution an additional dependence of the lumped transport coefficients arises that usually cannot be neglected. Profiles, which are calculated with constant lumped coefficients can be very inaccurate, especially when the transport-dispersive model is used. Hence, for moderate and low efficient systems the ''modifier'' dependence of the lumped coefficients should always be accounted for.

6. Nomenclature

a_p	external surface of adsorbent pellet: $a_p = \frac{6}{d_p}$ for spherical particles (m^2/m^3)
c	concentration in mobile phase ($kmol/m^3$)
c_p	concentration in the stagnant liquid phase ($kmol/m^3$)
C	dimensionless concentration in mobile phase
C_p	dimensionless concentration in the stagnant liquid phase
d_p	equivalent particle diameter (m)
D_{eff}	effective diffusion coefficient (m^2/s)
D_L	axial diffusion coefficient (m^2/s)
F_t	$=(1-\varepsilon_t)/\varepsilon_t$ phase ratio
F_e	$=(1-\varepsilon_e)/\varepsilon_e$
F_p	$=(1-\varepsilon_p)/\varepsilon_p$
H	Henry constant
k_0	retention factor of the component in the column
k_p	retention factor of the component in the particle
k_{ext}	external mass transport coefficient (m/s)
k_{ov}	overall mass transport coefficient (m/s)
k_m	lumped mass transport coefficient (m/s)
K_r	equilibrium constant ($m^3/kmol$)
L	column length (m)
m_{Kr}	parameters in Eqs. (5) and (6)
m_H	parameters in Eqs. (5) and (6)
m	moment of the chromatographic band profile
N^{eff}	number of theoretical plates [Eq. (20)]
N_{edm}	number of theoretical plates corresponding to the equilibrium-dispersive model
N_{grm}	number of theoretical plates corresponding to the general rate model
N_{tdm}	number of theoretical plates corresponding to the transport-dispersive model
p_{Kr}	parameters in Eqs. (5) and (6)
p_H	parameters in Eqs. (5) and (6)
q	adsorbed phase concentration (kmol/kg)
q_i^*	stationary phase concentration in equilibrium with the local stagnant mobile liquid concentrations (kmol/kg)
q_i^∞	loading capacity (kmol/kg)
Q	dimensionless adsorbed phase concentration
Q^*	dimensionless adsorbed phase concentration in equilibrium with the local stagnant liquid phase concentrations
r	radial coordinate (m)
R	dimensionless radial coordinate
t	time (s)
t_p	time of a rectangular pulse injection
u	superficial velocity (m/s)
w	$=u/\varepsilon_t=$interstitial velocity (m/s)
x	axial coordinate (m)
y	dimensionless concentration in mobile phase
y_p	dimensionless concentration or average dimensionless concentration in the stagnant mobile phase
z	dimensionless axial coordinate

Greek letters

ε_e, ε_p, ε_t	external, internal and total void fractions
μ	absolute error
μ'	central error
ρ_s	solid mass density (kg/m^3)
σ^2	variance (second central moment)

τ	dimensionless time
τ_p	dimensionless time of rectangular pulse injection

Subscripts

F	feed mod = modifier

Criterial numbers

Bi	Biot number, $k_{ext}d_p/2D_{eff}$
Pe	Peclet number, $uL/D_L\varepsilon_e$
Pe_a	apparent Peclet number
St	Stanton number, $k_{ext}a_pL\varepsilon_e/u$
St_m	lumped Stanton number, $k_m a_p L\varepsilon_e/u$
St_{ov}	overall Stanton number, $k_{ov}a_pL\varepsilon_e/u$

References

[1] D.M. Ruthven, Principles of Adsorption and Adsorption Process, John Wiley, New York, 1984.
[2] M. Suzuki, Adsorption Engineering, Elsevier, Amsterdam, 1990.
[3] G. Guiochon, S. Golshan-Shirazi, A.M. Katti, Fundamentals of Preparative and Non-linear Chromatography, Academic Press, Boston, MA, 1994.
[4] G. Guiochon, J. Chromatogr. A 965 (2002) 129.
[5] V.J. Villadsen, M.L. Michelsen, Solution of Differential Equation Model by Polynomial Approximation, Prentice-Hall, Englewood Cliffs, NJ, 1978.
[6] K. Kaczmarski, M. Mazzotti, G. Storti, M. Morbidelli, Comput. Chem. Eng. 21 (1997) 641.
[7] M. Morbidelli, A. Servida, G. Storti, S. Carra, Ind. Eng. Chem. Fundam. 21 (1982) 123.
[8] M. Morbidelli, G. Storti, S. Carra, G. Niederjaufner, A. Pontoglio, Chem. Eng. Sci. 39 (1984) 383.
[9] P. Sajonz, H. Guan-Sajonz, G. Zhong, G. Guiochon, Biotechnol. Prog. 12 (1997) 749.
[10] K. Miyabe, G. Guiochon, J. Chromatogr. A 866 (2000) 147.
[11] P. Rouchon, M. Schonauer, P. Valentin, G. Guiochon, Sep. Sci. Technol. 22 (1987) 1793.
[12] L.R. Snyder, J.W. Dolan, J. Chromatogr. 540 (1991) 21.
[13] L. Lapidus, N.L. Amundson, J. Phys. Chem. 56 (1952) 984.
[14] E. Kučera, J. Chromatogr. A 19 (1965) 237.
[15] D. Antos, Habilitation Thesis, University of Magdeburg, 2003.
[16] K. Kaczmarski, D. Antos, H. Sajonz, P. Sajonz, G. Guiochon, J. Chromatogr. A 925 (2001) 1.
[17] R.H. Perry, R.H. Green, J.O. Maloney, Chemical Engineers Handbook, 7th ed, McGraw-Hill, New York, 1997, Chapter 16.
[18] E. Soczewinski, Anal. Chem. 41 (1969) 179.
[19] L.R. Snyder, Anal. Chem. 46 (1974) 1384.
[20] D. Antos, W. Piatkowski, K. Kaczmarski, J. Chromatogr. A 874 (2000) 1.
[21] D. Antos, A. Seidel-Morgestern, Sep. Sci. Technol. 37 (7) (2002) 1469.
[22] E.J. Wilson, C.J. Geankoplis, Ind. Eng. Chem. Fundam. 5 (1966) 9.
[23] S.F. Chung, C.Y. Wen, AIChE J. 14 (1968) 857.
[24] G. Storti, M. Mazzotti, M. Morbidelli, S. Carra, AIChE J. 39 (1993) 471.
[25] M.W. Phillips, G. Subramanian, S.M. Cramer, J. Chromatogr. 454 (1988) 1.
[26] S. Golshan-Shirazi, B. Lin, G. Guiochon, J. Phys. Chem. 93 (1989) 6871.
[27] J.J. van Deemter, F.J. Zuiderweg, A. Klinkenberg, Chem. Eng. Sci. 5 (1956) 271.
[28] J.H. Knox, J. Chromatogr. Sci. 15 (1977) 352.
[29] J.C. Giddings, Unified Separation Science, Wiley, New York, 1991.
[30] G.A. Heeter, A.I. Liapis, J. Chromatogr. A 796 (1998) 157.
[31] H.-K. Rhee, N.R. Amundson, Chem. Eng. Sci. 27 (1972) 199.
[32] F.G. Helfferich, P.W. Carr, J. Chromatgr. A. 629 (1993) 97.
[33] P.N. Brown, A.C. Hindmarsh, G.D. Byrne, Variable-Coefficient Ordinary Differential Equation Solver; procedure available at http://www.netlib.org.